haematologica
Journal of the Ferrata Storti Foundation

HDAC6 inhibitors sensitize resistant t(11;14) multiple myeloma cells to a combination of bortezomib and BH3 mimetics

by Cristina Florean, Manon Lernoux, Anne Lorant, Helene Losson, Guy Bormans, Michael Schnekenburger, and Marc Diederich

HDAC6 inhibitors sensitize resistant t(11;14) multiple myeloma cells to a combination of bortezomib and BH3 mimetics

Cristina Florean[1], Manon Lernoux[1], Anne Lorant[1], Helene Losson[1], Guy Bormans[2], Michael Schnekenburger[1,*], Marc Diederich[3,*]

[1] Laboratoire de Biologie Moléculaire et Cellulaire du Cancer, Luxembourg, Luxembourg;

[2] Laboratory for Radiopharmaceutical Research, Department of Pharmaceutical and Pharmacological Sciences, KU Leuven, Leuven, Belgium;

[3] Research Institute of Pharmaceutical Sciences & Natural Products Research Institute, College of Pharmacy, Seoul National University, Seoul, Republic of Korea.

Running title: HDAC6 inhibitors for MM combination treatments.

* Co-corresponding authors:

Marc Diederich. Tel: +82-2-880-8919; E-mail address: marcdiederich@snu.ac.kr; College of Pharmacy, Seoul National University, Seoul, Republic of Korea.

Michael Schnekenburger. E-mail address: michael.schnekenburger@lbmcc.lu; Laboratoire de Biologie Moléculaire et Cellulaire du Cancer, Luxembourg, Luxembourg

Keywords: HDAC6 inhibitors, bortezomib, BH3 mimetics, multiple myeloma.

Author contributions: Cristina Florean and Manon Lernoux performed in vitro/*in cellulo* experiments; Anne Lorant performed, analyzed, and interpreted bioinformatic data and statistical analyses; Hélène Losson performed additional experiments; Guy Bormans synthesized the inhibitor; Cristina Florean, Michael Schnekenburger, and Marc Diederich conceived and designed the project. Cristina Florean, Michael Schnekenburger, Anne Lorant, and Marc Diederich wrote/edited the manuscript; Marc Diederich supervised the project. All authors have read and approved the manuscript.

Conflict of interest: The authors declare no conflict of interest.

Data-sharing statement

RNA-seq data were retrieved from the database of genotypes and phenotypes (dbGaP) under accession number phs000748.

CRISPR-Cas9 gene effect data were obtained from the Achilles project: https://doi.org/10.25452/figshare.plus.25880521.v1

Interested people can obtain additional information by contacting the corresponding authors.

The treatment landscape for multiple myeloma (MM) has evolved with proteasome inhibitors, steroids, immunomodulating drugs, monoclonal antibodies, CAR-T cells, and bispecific antibodies [1]. Despite advancements, therapeutic resistance remains a challenge. The pan-HDAC inhibitor (HDACi) panobinostat, approved for relapsed/refractory MM with bortezomib and dexamethasone [2], confirmed the potential of HDACi in MM treatment [3]. HDAC6i ricolinostat (ACY-1215) [4] and citarinostat showed promise in clinical trials with favorable toxicity profiles. Venetoclax emerged as an option for MM patients with t(11;14) or high Bcl-2 expression [5]. Mcl-1 inhibitors and B-cell maturation antigen (BCMA)-targeting agents are advancing, though durable remission remains elusive [6], underlining the need for innovative combination therapies. We combined HDAC6i with bortezomib and BH3 mimetics in MM subgroups. Additionally, we explored the impact of HDACi on BCMA expression to understand the effects on potential combination treatments. Our findings suggest that HDAC6i, in combination with bortezomib and BH3 mimetics, could benefit t(11;14) patients refractory to venetoclax.

Using transcriptomic data, we developed an HDAC6 activity score for MM patients, extending prior work in other cancers[7]. We analyzed a cohort of 655 MM patients from the MM Research Foundation (MMRF) CoMMpass dataset to identify subgroups potentially benefiting from HDAC6i. We used the algorithm for the reconstruction of accurate cellular networks (ARACNe) to construct a disease-specific gene regulatory network, extracting an HDAC6 regulon of 95 genes. A master regulator inference algorithm was used to calculate an HDAC6 activity score for each patient within this sub-network (Figure 1A) [7]. Our multivariate regression analysis indicated that "age" significantly affected the HDAC6 regulon scores, with younger patients having higher HDAC6 activity levels. Consequently, age was included as a covariate in the differential expression analysis. Enriched hallmark pathways associated with high HDAC6 scores-comprising the top tertile of patients-include interferon and interleukin 2 responses, MYC targets, and the unfolded protein response (UPR), indicating increased immune system activation, proliferation, and protein homeostasis and processing central to MM cell survival (Suppl. Figure 1A, left and middle panels). Further analysis of whole-genome CRISPR screening data revealed similar enrichment patterns in cell proliferation, oxidative phosphorylation (OXPHOS), and UPR categories (Suppl. Figure 1A, right panel). By integrating this score with recent multi-omics similarity network analyses [8], we identified distinct patient

subgroups with high HDAC6 scores, notably subgroup 3c [8], which frequently harbors the t(11;14) translocation and chromosome 1q amplification (Figure 1B, left panel). When dividing the HDAC6 scores into tertiles, we did not observe significant variations in BCL2 expression; a significant association was observed with MCL1 expression (Figure 1B, middle and right panels). To further explore these findings, we selected cell lines based on the presence of the t(11;14) translocation, expressing HDAC6 and Mcl-1. Whereas MOLP-8 expresses low levels of Bcl-2, U-266 expresses higher levels (Suppl. Table 1). Both cell lines showed increased α-tubulin acetylation after HDAC6 inhibition (Suppl. Figure 1B).

We characterized the effects of three HDAC6i (MAKV-15, tubastatin A, and ACY-1215) in MM cells. MAKV-15, an experimental tetrahydro-β-carboline analog of tubastatin A (compound 7) [9], demonstrated a lower IC_{50} for HDAC6 and adhered to Lipinski's rule of Five (data not shown). Our data confirmed that MAKV-15 is 26 times more potent and 3.4 times more selective against HDAC6 than tubastatin A, with IC_{50} values of 380 nM for HDAC1 and 29 nM for HDAC6, compared to tubastatin A's 2.9 µM and 0.75 µM, respectively (Figure 1C). Furthermore, MAKV-15's IC_{50} for HDAC6 is 1.5 times lower than that of ACY-1215 (21 and 31 nM, respectively). We evaluated the compounds' effects on α-tubulin and histone H4 acetylation in MOLP-8 and U-266 cell lines, which carry the t(11;14) translocation and 1q chromosome abnormalities [10]. The results demonstrated that MAKV-15 is more selective than tubastatin A and acts similarly to ACY-1215 regarding HDAC6 selectivity (Figure 1D and Suppl. Figure 1C). Kinetic analyses indicated that MAKV-15 exhibits more sustained activity than tubastatin A (Suppl. Figure 1D).

MAKV-15, tubastatin A, and ACY-1215 induced growth inhibition (GI) at HDAC6-selective doses in MOLP-8 and U-266 cells, with respective GI_{50} values of 13.25 ± 5.3 µM, 3.19 ± 3.55 µM, and 1.2 ± 0.29 µM for MOLP-8; 6.01 ± 2.41 µM, 0.38 ± 0.66 µM, and 0.973 ± 0.2 µM for U-266. Apoptosis was observed at non-HDAC6-selective concentrations (Suppl. Figure 2A), indicating that HDAC6 inhibition is cytostatic rather than cytotoxic for these cells and supporting the potential of HDAC6i in combination treatments.

Given the warning about panobinostat's cardiac toxicity, we assessed the cardiac effects of

4

HDAC6i using SeeSAR, PredhERG, and SwissDock to predict the likelihood of compounds blocking the ether-a-go-go-related gene (hERG) cardiac potassium channel, a key anti-target for HDACi. MAKV-15 and tubastatin A showed no interactions via SeeSAR and PredhERG, with ΔG values of -7.73 and -6.96 kcal/mol, respectively, from SwissDock. Ricolinostat (ACY-1215) and citarinostat (ACY-241) also showed no interactions across all tools. Panobinostat showed interactions in the μM-mM range by SeeSAR, weak/moderate by PredhERG, and a ΔG of -6.43 kcal/mol. Suberoylanilide hydroxamic acid (SAHA) showed interactions in the μM-mM range by SeeSAR, none by PredhERG, and a ΔG of -6.33 kcal/mol. These findings suggest that HDAC6i may have a safer cardiac profile than pan-HDACi.

MAKV-15 induced α-tubulin acetylation across an extended panel of MM cell lines (Suppl. Figure 1B), independent of HDAC6 expression levels (Suppl. Figure 1E). The effectiveness of MAKV-15 in acetylating α-tubulin shows that its inhibitory action on HDAC6 is robust enough to override differences in HDAC6 expression, ensuring reduced activity of HDAC6 across cell lines.

To assess proteotoxic stress, we tested HDAC6i in combination with bortezomib in MOLP-8 cells, observing the accumulation of ubiquitinated proteins (Figure 1E) and augmented apoptosis in both MOLP-8 and U-266 (Figure 1F and Suppl. Figure 2C). Additionally, neither MAKV-15 (up to 50 μM) nor its combination with bortezomib at subtoxic doses affected the viability of peripheral blood mononuclear cells (PBMCs) from healthy donors (Suppl. Figure 2B). PBMCs were used with the approval of the National Research Ethics Committee of Luxembourg and were isolated from blood obtained from the Red Cross Luxembourg.

We then assessed the effect of triple treatments with bortezomib, MAKV-15 or ACY-1215, and a BH3 mimetic (Bcl-2 inhibitor venetoclax or Mcl-1 inhibitors S63845 and A210477) on MM cell viability, focusing on MOLP-8 and U-266 cells, which bear the t(11;14) translocation but are resistant to venetoclax [10], compared with the non-t(11;14) KMS-28-BM cells. We found that triple therapies significantly increased apoptosis in MOLP-8 cells compared to double treatments, as evidenced by nuclear morphology analysis (Figure 2A) along with pro-caspase 3 and PARP-1 cleavage (Figure 2B). Combination index (CI) analysis for the MAKV-15/

bortezomib/venetoclax triple therapy showed synergism (CI=0.597) (data not shown) at the doses used in Figure 2A-B. In U-266 cells, only the triple therapies with bortezomib, MAKV-15, and S63845 significantly enhanced cell death compared to double treatments (Figure 2A). Finally, KMS-28-BM cells were less affected by triple therapies, showing no significant difference from double combinations (Suppl. Figure 2E).

Western blot analyses revealed no changes in Bcl-2 and Bcl-xL levels, while Mcl-1 levels decreased after treatment with bortezomib and HDAC6i (Figure 2B). These results support the role of Mcl-1 in MM resistance, justifying ongoing clinical trials with Mcl-1 inhibitors. The reduction of Mcl-1 by HDAC6i plus bortezomib could sensitize venetoclax-resistant t(11;14) cells. Moreover, HDAC6i decreased c-Myc levels accompanied by increased K148 acetylation (Figure 2C), consistent with observations in breast cancer [7]. Inhibiting c-Myc degradation impairs its pro-proliferative activity [12], suggesting that combining HDAC6i with proteasome inhibitors could lead to inactive c-Myc complexes and impaired proliferation.

Finally, we explored the effects of HDACi on BCMA expression levels, the target of a new promising therapeutic class. Network analysis revealed that HDAC1 is closely connected to BCMA in the interaction network constructed from MMRF CoMMpass datasets, while HDAC6 is more distantly connected (Figure 3A, left panel). Moreover, the HDAC6 score does not correlate with BCMA expression in MM patients (Figure 3A, right panel). Previous data showed that SAHA decreased BCMA gene expression [13]. Consistently, our experiments showed that BCMA protein levels decreased in MM cells upon treatment with pan-HDACi but not HDAC6i (Figure 3B).

To assess BCMA surface expression levels, we co-treated cells with the gamma-secretase inhibitor RO4929097 to prevent protein shedding. Treatment with SAHA and panobinostat almost abolished surface BCMA (range: 67 to 91% reduction), while MAKV-15 and ACY-1215 only mildly affected its levels (range: 18 to 41% reduction) (Figure 3C and Supplementary Figure 2F). These findings align with previous reports [13, 14] and suggest a dual mechanism of HDAC-related BCMA control: total expression is affected by pan-HDACi, while HDAC6i may influence surface trafficking. This indicates a need for careful evaluation before using these

agents in combination therapies.

In conclusion, our study identified a subgroup of MM patients with high HDAC6 activity, suggesting that HDAC6i combined with bortezomib and BH3 inhibitors can target specific MM subtypes. We demonstrated that HDAC6i has less impact on BCMA levels than pan-HDAC inhibitors. Overall, our data highlights the potential of HDAC6i in combination therapies for t(11;14) patients. Our findings support further exploration of HDAC6i-based regimens to optimize therapeutic outcomes for MM patients.

References

1. Monteith BE, Sandhu I, Lee AS. Management of Multiple Myeloma: A Review for General Practitioners in Oncology. Curr Oncol. 2023;30(5):4382-4401.

2. Yee AJ, Raje NS. Panobinostat and Multiple Myeloma in 2018. Oncologist. 2018;23(5):516-517.

3. Imai Y, Hirano M, Kobayashi M, Futami M, Tojo A. HDAC Inhibitors Exert Anti-Myeloma Effects through Multiple Modes of Action. Cancers (Basel). 2019;11(4):475.

4. Vogl DT, Raje N, Jagannath S, et al. Ricolinostat, the First Selective Histone Deacetylase 6 Inhibitor, in Combination with Bortezomib and Dexamethasone for Relapsed or Refractory Multiple Myeloma. Clin Cancer Res. 2017;23(13):3307-3315.

5. Lernoux M, Schnekenburger M, Dicato M, Diederich M. Susceptibility of multiple myeloma to B-cell lymphoma 2 family inhibitors. Biochem Pharmacol. 2021;188:114526.

6. Zhou X, Rasche L, Kortum KM, Mersi J, Einsele H. BCMA loss in the epoch of novel immunotherapy for multiple myeloma: from biology to clinical practice. Haematologica. 2023;108(4):958-968.

7. Zeleke TZ, Pan Q, Chiuzan C, et al. Network-based assessment of HDAC6 activity predicts preclinical and clinical responses to the HDAC6 inhibitor ricolinostat in breast cancer. Nat Cancer. 2023;4(2):257-275.

8. Bhalla S, Melnekoff DT, Aleman A, et al. Patient similarity network of newly diagnosed multiple myeloma identifies patient subgroups with distinct genetic features and clinical implications. Sci Adv. 2021;7(47):eabg9551.

9. Butler KV, Kalin J, Brochier C, Vistoli G, Langley B, Kozikowski AP. Rational design and simple chemistry yield a superior, neuroprotective HDAC6 inhibitor, tubastatin A. J Am Chem Soc. 2010;132(31):10842-10846.

10. Ziccheddu B, Da Via MC, Lionetti M, et al. Functional Impact of Genomic Complexity on the Transcriptome of Multiple Myeloma. Clin Cancer Res. 2021;27(23):6479-6490.

11. Shultz MD, Cao X, Chen CH, et al. Optimization of the in vitro cardiac safety of hydroxamate-based histone deacetylase inhibitors. J Med Chem. 2011;54(13):4752-4772.

12.   Jaenicke LA, von Eyss B, Carstensen A, et al. Ubiquitin-Dependent Turnover of MYC Antagonizes MYC/PAF1C Complex Accumulation to Drive Transcriptional Elongation. Mol Cell. 2016;61(1):54-67.

13.   Mitsiades CS, Mitsiades NS, McMullan CJ, et al. Transcriptional signature of histone deacetylase inhibition in multiple myeloma: biological and clinical implications. Proc Natl Acad Sci U S A. 2004;101(2):540-545.

14.   Ramkumar P, Abarientos AB, Tian R, et al. CRISPR-based screens uncover determinants of immunotherapy response in multiple myeloma. Blood Adv. 2020;4(13):2899-2911.

Figure Legends

Figure 1. Histone Deacetylase (HDAC)6 Score Analysis Identifies multiple myeloma (MM) Patient Subgroups for Studying the Effects of HDAC6 Inhibitors. A) Overview of HDAC6 score construction. RNA-seq data from 655 newly diagnosed MM patients were analyzed using the Algorithm for the Reconstruction of Accurate Cellular Networks (ARACNe) algorithm to reconstruct signaling interactomes. The HDAC6 regulon was identified by extracting its first neighbors within the MM-specific network, and activity scores were calculated. These scores were then Z-transformed within the cohort. **B)** HDAC6 score distribution across different MM patient subgroups. The left panel shows a boxplot of HDAC6 Z-scores across different subgroups, with the horizontal dashed line representing the overall mean. The middle and right panels show B-cell lymphoma (BCL)2 and myeloid cell leukemia (MCL)1 expression levels in the HDAC6 score tertiles, respectively, with dashed lines indicating mean expression levels. Wilcoxon tests compared subgroups against the overall mean in all plots, with p-values adjusted using the false discovery rate (FDR) method. **C)** Comparative analysis of the inhibitory effects of MAKV-15, tubastatin A, and ACY-1215 on HDAC1 and HDAC6. HDAC activity assays were conducted with various concentrations of MAKV-15 and tubastatin A. Data represent the percentage of residual activity relative to the control. **D)** Western Blot analysis of acetyl-α-tubulin and acetyl-histone 4 in MOLP-8 cells. Cells were treated for 24 hours with increasing concentrations of MAKV-15, tubastatin A, or ACY-1215. β-actin and Histone 1 were used as loading controls. Suberoylanilide hydroxamic acid (SAHA; 2 µM) was used as a reference pan-HDAC inhibitor. **E)** Effects of combined inhibition of HDAC6 and the proteasome on MM cells. Western blot analysis showed ubiquitinated proteins in MOLP-8 cells treated as indicated, using β-actin as a loading control. Immunoblots are representative of three independent experiments. **F)** Annexin V and propidium iodide (PI) staining followed by FACS analysis in MOLP-8 and U-266 cells. Cells were treated with MAKV-15 (5 µM) and bortezomib (5 nM for MOLP-8 and 2.5 nM for U-266) for 72 hours. Graphs show the mean ± standard deviation (SD) of Annexin V-positive plus double Annexin V- and PI- positive cells from three independent experiments. Statistical significance was determined using one-way Analysis of Variance (ANOVA) with Holm-Šidák's multiple comparison test, comparing each sample to the control. * $p \leq 0.05$; ** $p \leq 0.01$; *** $p \leq 0.001$. Abbreviations in the figure: MMRF (Multiple Myeloma Research

Foundation), CCDN1 (cyclin D1), MMSET (multiple myeloma Su(var)3-9, Enhancer-of-zeste and Trithorax (SET) domain), MAF (musculoaponeurotic fibrosarcoma oncogene homolog), HD (hyperdiploidy).

Figure 2. Combination Treatments of HDAC6 Inhibitors with Bortezomib and BH3 Mimetics Reduce t(11;14) Cell Viability. A) Apoptosis induction analysis. Nuclear morphology analyses were conducted on MOLP-8 and U-266 cells treated with 5 µM MAKV-15, subtoxic concentrations of bortezomib (MOLP-8: 5 nM; U-266: 2.5 nM), venetoclax (5 µM), A1210477 (MOLP-8: 1 µM; U-266: 5 µM), S63845 (MOLP-8: 10 nM; U-266: 100 nM), or combinations of these drugs for 72 hours. Data represent the mean ± SD of three to five independent experiments. Statistical analysis shows the significance of triple treatments compared to all three corresponding double treatments. ** $p \leq 0.01$; *** $p \leq 0.001$. One-way ANOVA with Holm-Šidák's multiple comparison test. **B)** Western Blot analysis of caspase-3, poly (ADP-ribose) polymerase (PARP)-1 cleavage, and Bcl-2 family protein members in MOLP-8 and U-266 cells treated with the indicated drugs at concentrations as in panel A. **C)** Western Blot analysis of total and acetylated (K148ac) c-Myc in MOLP-8 cells. Cells were treated with MAKV-15 or ACY-1215 for 24 hours. Immunoblot images are representative of three independent experiments. Abbreviations in the figure: Mcl-1 (myeloid cell leukemia), Bcl-2 (B-cell leukemia/lymphoma-2), Bcl-xL (B-cell lymphoma extra-large).

Figure 3. Pan-HDAC Inhibitors Decrease Total and Surface B-cell maturation antigen (BCMA) Levels in MM Cells. A) Interaction network between HDAC isoforms and BCMA. The left panel illustrates the network, while the right panel shows a scatter plot indicating no correlation between HDAC6 activity scores and BCMA expression in the Relating Clinical Outcomes in Multiple Myeloma to Personal Assessment of Genetic Profile (CoMMpass) patient cohort. The Pearson correlation coefficient and corresponding p-value are displayed. **B)** Western Blot analysis of BCMA in MOLP-8 and MM.1S Cells. Cells were treated for 24 hours with HDAC6i (5 µM MAKV-15, 1 µM ACY-1215, 1 µM nexturastat A, 2 µM tubacin, 5 µM tubastatin A) or pan-HDAC inhibitors [2 µM suberoylanilide hydroxamic acid (SAHA) and 10 nM panobinostat] (left panel), and MOLP-8 cells were treated with increasing concentrations of MAKV-15 and ACY-1215 for 24 hours (right panel). Immunoblot images are representative of

three independent experiments. **C)** FACS analysis of BCMA surface expression levels in MOLP-8 cells. Cells were co-treated with the gamma-secretase inhibitor RO4929097 and pan-HDAC or HDAC6i for 24 hours. Representative histograms are shown (left panel), with corresponding quantifications (right panel). Graphs represent the mean ± SD of BCMA median fluorescence intensity (MFI) levels from three independent experiments. *** $p \leq 0.001$. One-way ANOVA with Holm-Šidák's multiple comparison test was used to compare each sample; statistical significance was determined for comparisons with the control sample and indicated pairs of samples.
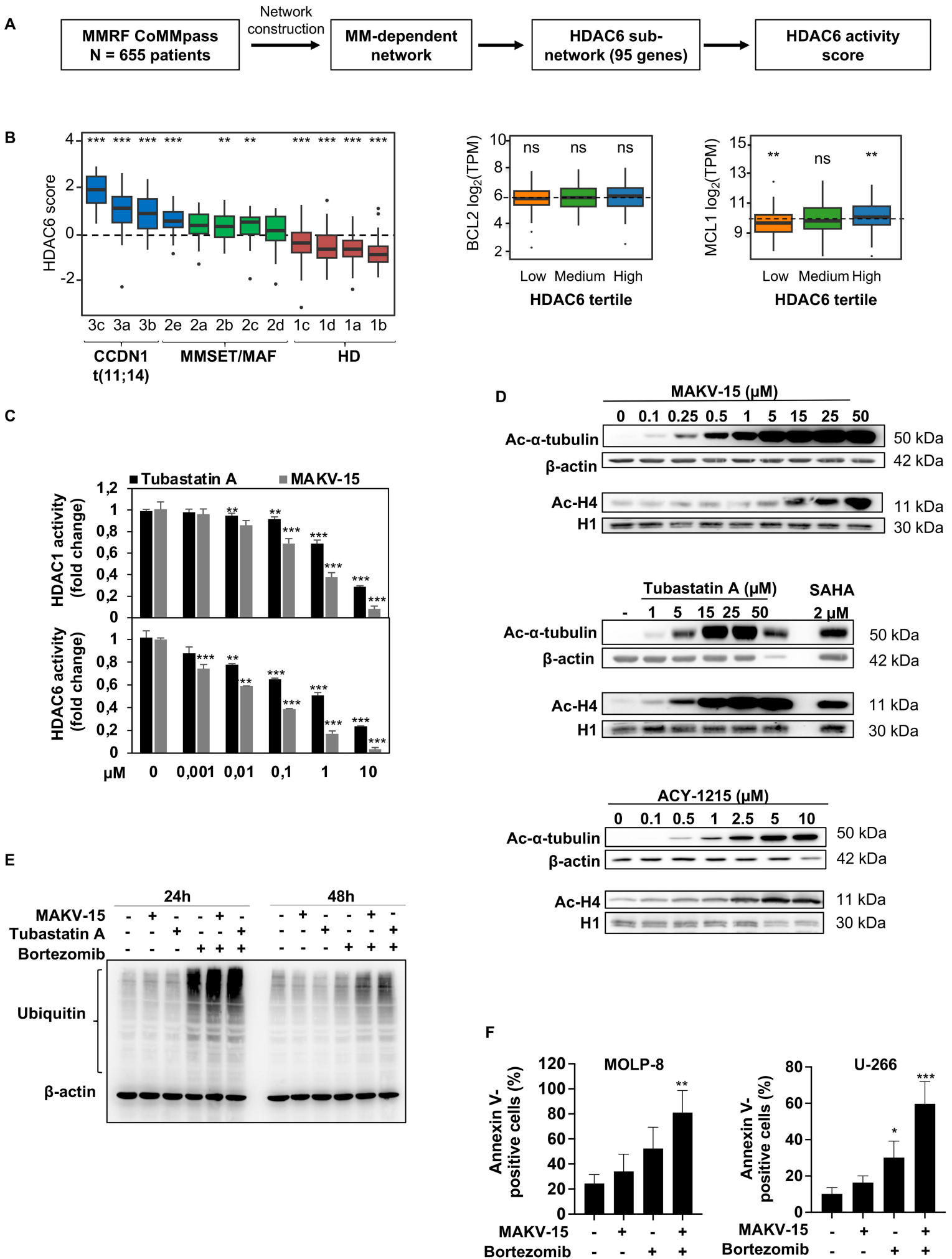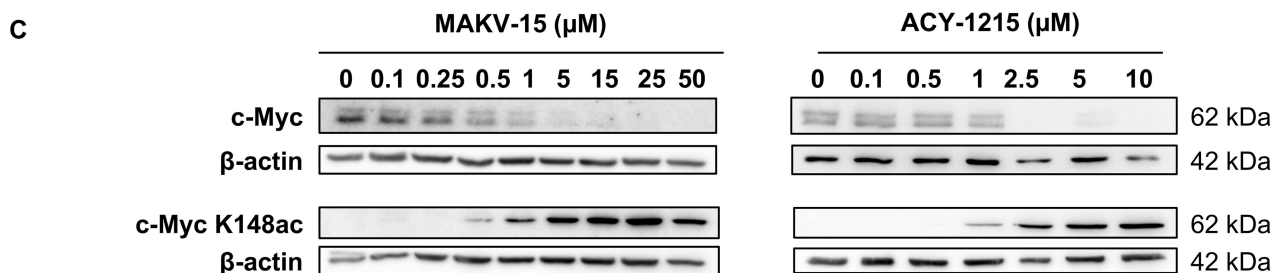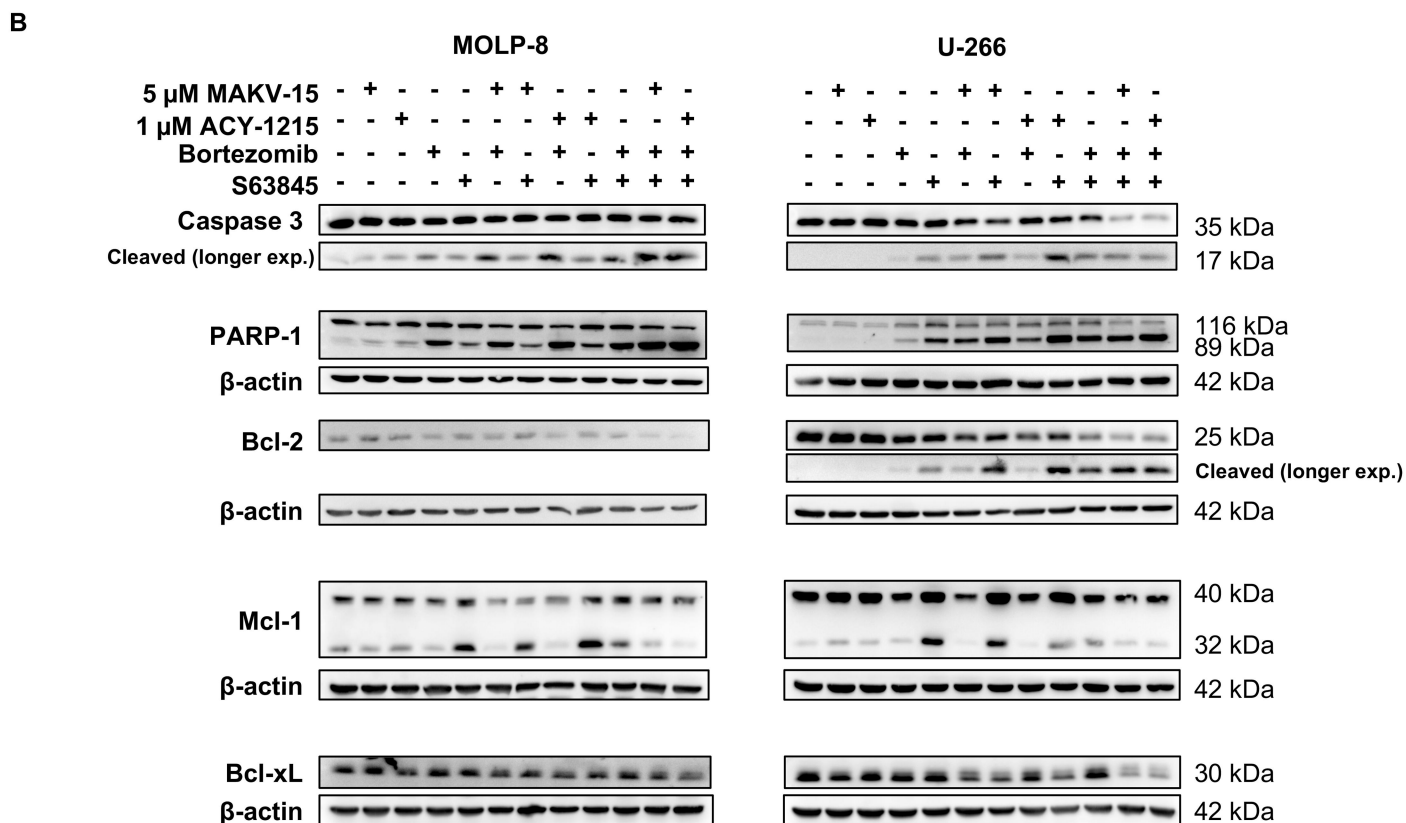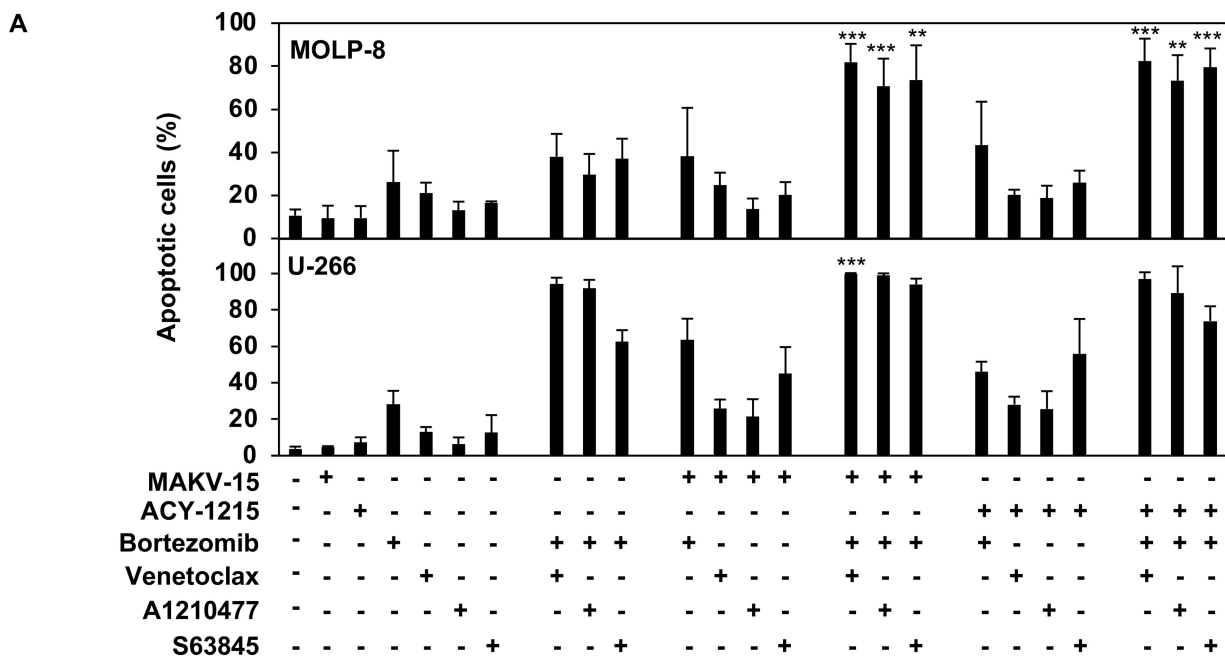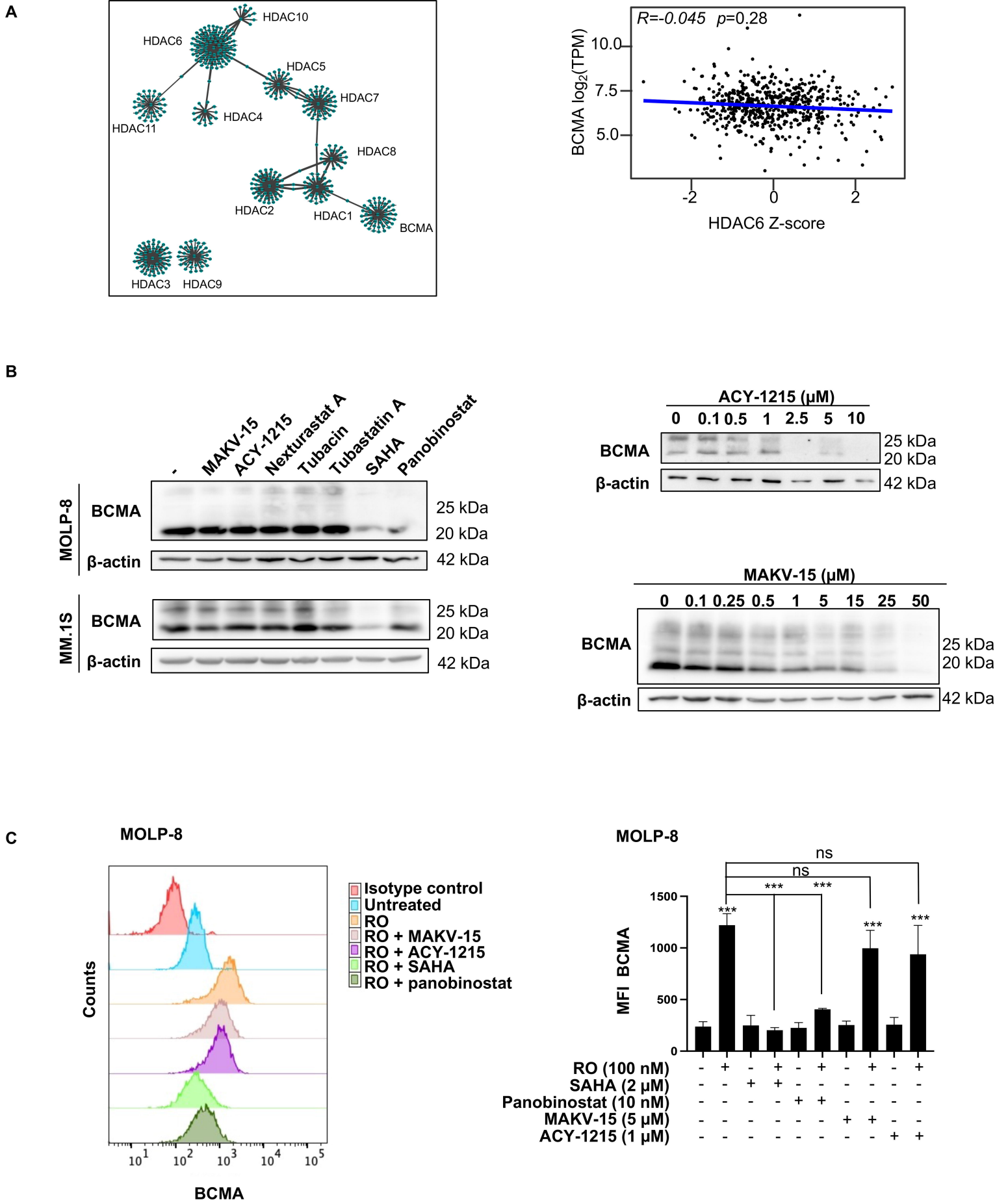
Figure 1

Figure 2

Figure 3

Supplementary Materials

HDAC6 inhibitors sensitize resistant t(11;14) multiple myeloma cells to a combination of bortezomib and BH3 mimetics

Cristina Florean[1], Manon Lernoux[1], Anne Lorant[1], Helene Losson[1], Guy Bormans[2], Michael Schnekenburger[1,*], Marc Diederich[3,*]

Supplementary Figure Legends

Supplementary Figure 1. MAKV-15 is Effective in a Panel of multiple myeloma (MM) Cell Lines Without Correlation with histone deacetylase (HDAC)6 Expression Levels. A) Differential gene expression and pathway enrichment analysis in high vs low HDAC6 score patients. The left panel shows a volcano plot of differentially expressed genes between the high and low tertiles of HDAC6 activity scores in MM patients. Genes with a |log2 fold change > 0.3 and a false discovery rate (FDR) < 0.05 were considered significantly different. The middle panel depicts enriched hallmark pathways associated with high HDAC6 scores. The left panel depicts pathways enriched for genes negatively influencing MM cell line proliferation from whole genome CRISPR screening. **B)** Western blot analyses for ac-α-tubulin and ac-H4 in a panel of MM cell lines treated with 5 μM MAKV-15 for up to 48h. β-actin and Histone 1 (H1) were used as loading controls. Suberoylanilide hydroxamic acid (SAHA; 2 μM) was used as a reference pan-HDACi. **C)** Western blot analyses for acetyl (ac)-α-tubulin and ac-Histone 4 (H4) in U-266 cells treated for 24h with increasing concentrations of MAKV-15, tubastatin A, or ACY-1215. **D)** Kinetic western blot analysis of ac-α-tubulin and ac-H4 in MOLP-8 cells treated for up to 72h with MAKV-15 or tubastatin A. **E)** Western blot analysis of HDAC6 expression levels in the panel of MM cell lines used. Immunoblots are representative of three independent experiments. Abbreviations in the figure: OXPHOS (oxidative phosphorylation).

Supplementary Figure 2. Effect of MAKV-15, Tubastatin A, and ACY-1215 on MM Cell Viability. A) The viability of MOLP-8 and U-266 cells was assessed by nuclear morphology analysis upon treatment with the indicated concentrations of MAKV-15, tubastatin A, and ACY-

1215 for up to 72h. **B)** Non-proliferative and proliferative peripheral blood mononuclear cells (PBMCs) were treated with the drugs alone or in combinations as described in the figures. After the indicated incubation time, cell viability was assessed using a Trypan blue-exclusion analysis. PBMCs and P_PBMCs were used with the approval of the National Research Ethics Committee of Luxembourg. PBMCs were isolated from blood obtained from the Red Cross (Luxembourg, Luxembourg) under the authorization LBMCC-2019-0002: "Assessment of toxicity of new drugs or drug combinations in preclinical development in nonproliferating peripheral blood mononuclear cells (systemic acute toxicity)". P_PBMCs were generated from blood obtained from the Red Cross under the authorization LBMCC- 2019-0001: "Assessment of differential toxicity of new drugs or drug combinations in preclinical development in *ex-vivo* proliferating peripheral blood mononuclear cells vs. proliferating cancer cells." **C)** Nuclear morphology analysis of MOLP-8 cells treated with the indicated compounds for 72h. **D)** Western blot analysis of caspase-3, poly (ADP-ribose) polymerase (PARP)-1 cleavage in MOLP-8 treated with the indicated drugs. **E)** Nuclear morphology analysis (upper panel) and Western blot analysis of caspase 3, PARP-1, and Bcl-2 family protein members (lower panel) in KMS-28-BM cells treated with the indicated drugs for 72h. Images are representative of three independent experiments. Graphs correspond to the mean ± SD of three independent experiments. The selected statistical analysis reports the significance of triple treatments compared to all the corresponding double treatments. **F)** FACS analysis of B-cell maturation antigen (BCMA) surface expression levels in MM.1S cells. Cells were co-treated with the gamma-secretase inhibitor RO4929097 and SAHA or MAKV-15 for 24 hours. Graphs represent the mean ± SD of BCMA median fluorescence intensity (MFI) levels from three independent experiments. * $p \leq 0.05$; ** $p \leq 0.01$; *** $p \leq 0.001$. One-way ANOVA with Holm-Šidák's multiple comparison test was used to compare each sample; statistical significance was determined for comparisons with the control sample and indicated pairs of samples.

Supplemental Table 1: Molecular features and key genetic aberrations in multiple myeloma cell lines. [1-3]

Cell Line	Relative HDAC6 Expression	Relative Mcl-1 Expression	Bcl-2 Expression	t(11;14) Translocation	Origins and Characteristics
AMO-1	++	++++	High	unknown	Ascitic fluid of a 64-year-old woman with plasmacytoma (IgAkappa); coexpression of a CD4 antigen and plasma cell antigens (CD38 and PCA-1)
KMS-12-PE	+++	+++	High	+	Pleural effusion of a 64-year-old woman with refractory, terminal multiple myeloma
KMS-34	+++	+++	Low	unknown	Pleural effusion
MM.1S	++	++	High	-	B lymphoblast cell that was isolated from the peripheral blood of a Black, 42-year-old, female patient with immunoglobulin A lambda myeloma
MOLP-8	++	+++	Low	+	Peripheral blood of a 52-year-old man with multiple myeloma (stage IIIA, type IgD lambda)
JJN-3	+	++	High	-	Bone marrow of a 57-year-old woman with plasma cell leukemia (IgA1kappa)
KMS-28-BM	++++	+	High	-	Plasma Cell Myeloma
OPM-2	+++	++	High	-	Peripheral blood of a 56-year-old woman with multiple myeloma (IgG lambda) in leukemic phase (relapse, terminal)
MM.1R	++	++	High	-	B lymphoblast cell line that was isolated in 1990 from the peripheral blood of a 42-year-old, Black female with multiple myeloma who had become resistant to steroid-based therapy
U-266	++	+++	High	+	Peripheral blood of a 53-year-old man with IgE-secreting myeloma (refractory, terminal)

Supplementary References

1.   Punnoose EA, Leverson JD, Peale F, et al. Expression Profile of BCL-2, BCL-XL, and MCL-1 Predicts Pharmacological Response to the BCL-2 Selective Antagonist Venetoclax in Multiple Myeloma Models. Mol Cancer Ther. 2016;15(5):1132-1144.

2.   Trudel S, Li ZH, Rauw J, Tiedemann RE, Wen XY, Stewart AK. Preclinical studies of the pan-Bcl inhibitor obatoclax (GX015-070) in multiple myeloma. Blood. 2007;109(12):5430-5438.

3.   Jernberg-Wiklund H. Multiple Myeloma Cell Lines. Human Cell Culture, 2006:81-155.